

A Study of Numerical Methods for Solving Viscous and Inviscid Flow Problems*

T. D. TAYLOR, E. NDEFO, AND B. S. MASSON

Northrop Corporate Laboratories, Hawthorne, California

Received April 27, 1971

The numerical methods of Rusanov, Godunov, Richtmeyer and MacCormack are used to integrate the $1 - D$ equations of inviscid fluid flow for shock waves, contact surfaces and rarefaction waves. The results from each scheme are compared with the exact solutions to establish the accuracy. The results demonstrate that the method of Godunov and the third-order scheme of Rusanov have the optimum overall performance. For viscous flows the inviscid schemes of Rusanov were combined with explicit, implicit and Dufort-Frankel differencing of the viscous terms to integrate Burgers equation. The numerical results are compared with the exact solution and the error is tabulated.

1. INTRODUCTION

In recent years selection of a numerical method for solving the equations of viscous or inviscid fluid flow has become a difficult task due to the large number of finite difference schemes which are available. This task is often complicated by the fact that a scheme has been successfully applied to a problem without numerical difficulty, but the accuracy is not clearly established. As a result one cannot be sure of a method when applying it to another problem. Due to these uncertainties, the authors undertook a study of existing finite difference methods for solving fluid flow problems, with the intent of establishing optimum methods for computing inviscid and viscous flows. The study was limited to unsteady methods for calculation of steady-state flows. In the investigation the unsteady portion of the calculation is included to stabilize the difference method, and accuracy in calculating the transient is not emphasized. As a consequence, when accuracy is discussed it refers primarily to the steady state.

In order to evaluate the various types of difference methods it was necessary to

* The viscous portion of this work was supported by the Office of Naval Research under Contract N00014-70-0034 and the inviscid part was supported by Picatinny Arsenal under Contract DAAG07 69-C-0739.

select test cases with known solutions which were in some manner representative of flow problems. For the inviscid flow tests, the one-dimensional propagation of a shock wave, a rarefaction wave and a contact surface were selected for calculation by first-, second- and third-order finite difference methods. The results obtained from differencing the inviscid equations by the various methods were compared with the exact inviscid solutions. The results of these comparisons are discussed in the section on inviscid flows.

For the viscous flow tests, the nonlinear Burgers equation was employed as the model to be integrated. Various schemes which resulted from extending the inviscid methods to viscous calculations were tested. The methods ranged from first to third order depending on the magnitude of the Reynolds number. The numerical results were compared with the exact solution for a shock wave type flow. These are discussed in the section on viscous flows.

It is important to note that tests on both types of flows were conducted only in one space dimension and, therefore, sweeping conclusions for multidimensional problems cannot in general be made. If, however, a multidimensional problem can be reduced to unsteady one-dimensional operators by splitting [1-3] then the one-dimensional tests provide direct insight into the selection of a differencing method.

2. INVISCID METHODS

The critical test of any finite difference method for calculating inviscid flows is its performance in the vicinity of a steep flow gradient. If a method is stable and accurate when encountering shock waves, strong rarefactions and contact surfaces, it then can be expected to compute complex flows without numerical difficulties. Most methods unfortunately exhibit large errors in the vicinity of steep gradients or become completely unstable. In an effort to provide a basis for choosing one method over another for a particular problem, Emery [4] evaluated the methods of Lax [5], Rusanov [6] (1st order), Lanshoff [7], Lax-Wendroff [8] and Richtmyer [9]. From this study Emery chose the first-order scheme of Rusanov to be preferable to that of Lax or Lax-Wendroff. Unfortunately, Emery did not test the methods of Godunov [10], MacCormack [11] or Rusanov [12] (3rd order). In an attempt to evaluate these techniques and provide comparisons with Emery's investigation, a study of five different finite difference methods was undertaken. The methods were those of Godunov, Richtmyer, MacCormack and two by Rusanov. The numerical schemes all have the capability of smearing inviscid flow discontinuities into smooth profiles at least several mesh points wide. This smoothing property permits them to automatically compute flows with internal shock waves and contact discontinuities. The resulting smoothed jumps move with the correct speed and satisfy the actual inviscid jump conditions. All schemes are explicit, but differ in

order of accuracy, two being of first-order, two of second-order, and one of third-order accuracy.

In the study a series of numerical experiments was conducted to illustrate the magnitude and structure of the truncation viscosity produced by each scheme under several flow situations. The truncation viscosity is defined as the total numerical error composed of both the implicit truncation error associated with the differencing technique and any explicit artificial viscosity which might be added to the finite difference equations for stability. It is this total error term which governs the smearing of flow discontinuities into smooth variations. The implicit portion exists in all difference schemes, while the explicit portion may or may not be necessary. For example, explicit artificial terms appear in the two Rusanov methods, which are unstable without their use, but explicit terms do not appear in the Richtmyer method, which is stable without them. The other two methods studied are also stable without explicit artificial viscosity.

For comparison purposes each scheme was used to compute a rarefaction wave, a contact discontinuity and a shock wave. Each of these flows represents a different balance of the conservation laws with the truncation viscosity induced by the finite difference approximation. In a rarefaction wave, nonlinearity produces a spreading of the wave and all gradients decrease in magnitude with time. The truncation error also decreases and eventually becomes negligible. The magnitude of the truncation error can be verified by comparison with the analytical wave expressions. By contrast, a uniformly translating contact discontinuity is in dynamic equilibrium, and there is no nonlinear convection present to steepen or broaden disturbances. The contact discontinuity is modified and dominated entirely by the truncation viscosity. Finally, in the shock wave, the nonlinear effects tend to steepen the profile and the gradients increase in magnitude until the truncation viscosity is no longer negligible. Eventually a balance is established between the steepening caused by convection terms and the diffusion caused by truncation viscosity.

2.1. *Inviscid Numerical Procedures*

The numerical schemes which were tested approximate an equation of the form

$$w_t + f_x = 0, \quad (1)$$

where f is a function of w . Each scheme provides a "receipt" for calculating the value f_x and w_t from an initial distribution of w . The derivation of these procedures for computing derivatives in each case requires detailed analysis and as a result no attempt is made to reproduce these details in this paper. For the purposes of this discussion we will state each scheme in the form in which it was employed and compare the results of the various schemes.

TABLE I
Inviscid Finite Difference Methods

Originator	Order of accuracy	Abbreviation	Scheme	Stability condition
Godunov [10]	1	G	$w_m^{n+1} = w_m^n - q(f_{m+1/2}^{n+1/2} - f_{m-1/2}^{n+1/2}).$ $f_{m+1/2}^{n+1/2}$ is computed by formula for breakdown of a discontinuity. See reference [10].	$\sigma \leq 1$
Rusanov [6]	1	R1	$w_m^{n+1} = w_m^n - (q/2)(f_{m+1}^n - f_{m-1}^n) + (1/2)(\phi_{m+1/2}^n - \phi_{m-1/2}^n),$ $\phi_{m+1/2}^n = (1/2)(\alpha_{m+1}^n + \alpha_m^n)(w_{m+1}^n - w_m^n)$ $\alpha_m^n = \omega q(u + c)_m^n.$	$\sigma \leq \omega \leq \frac{1}{\sigma}, \sigma \leq 1$ ($\omega = 1.0$ and $\sigma = 0.95$ gave best results)
MacCormack [11]	2	MLW	$w_m^{n+1} = w_m^n - q(f_{m+1/2}^{n+1/2} - f_{m-1/2}^{n+1/2}),$ $f_{m+1/2}^{n+1/2} = (f_{m+1}^n + f_m^{n+1})/2,$ $f_{m-1/2}^{n+1/2} = w_m^n - q(f_{m+1}^n - f_m^n).$	$\sigma \leq 1$
Richmeyer [9]	2	RLW	$w_m^{n+1} = w_m^n - q(f_{m+1/2}^{n+1/2} - f_{m-1/2}^{n+1/2}),$ $w_m^{n+1/2} = (w_m^n + w_{m+1}^n)/2 - q(f_{m+1}^n - f_m^n)/2.$	$\sigma \leq 1$
Rusanov [12]	3	R3	$w_m^{n+1} = w_m^n - \omega(w_{m+2}^n - 4w_{m+1}^n + 6w_m^n - 4w_{m-1}^n + w_{m-2}^n)/24$ $+ \frac{1}{4} \{ (q/6)(-f_{m+2}^n + 7f_{m+1}^n - 7f_{m-1}^n + 2f_{m-2}^n) \}$ $+ \frac{3}{4} \{ (q/2)(f_{m+1}^{(2)} - f_{m-1}^{(2)}) \},$ $w_m^n = w_m^n + (2/3)q(f_{m+1/2}^{(1)} - f_{m-1/2}^{(1)}),$ $w_{m+1/2}^{(1)} = (1/2)(w_{m+1}^n + w_m^n) + (1/3)q(f_{m+1}^n - f_m^n).$	$4\sigma^2 - \sigma^4 \leq \omega \leq 3$ $\sigma \leq 1$ ($\omega = 2.0$ and $\sigma = 0.7$ gave best results)

Note: $q = \tau/h$ and $\sigma = (\tau/h)(u + c)_{\max}$

The tests of the five different numerical schemes listed in Table I were conducted for the one dimensional unsteady flow of an ideal gas. For this type of flow Eq. (1) can be written in a vector form in which w and f are the vector functions.

$$w = \begin{pmatrix} \rho \\ m \\ E \end{pmatrix} \quad f = \begin{pmatrix} \rho u \\ p + \rho u^2 \\ u(E + p) \end{pmatrix}.$$

The mass flux m and the fluid energy E are defined in terms of density, fluid velocity and pressure by the relations

$$m = \rho u$$

$$E = p/(\gamma - 1) + \rho u^2/2.$$

This form of Eq. (1) was integrated by each method for a standard set of initial conditions and the results obtained will be discussed next.

2.2. Numerical Results

The numerical calculations for the three wave propagation tests were conducted for the conditions shown in Table II. The state designated with the subscript 1 is located at the right-hand side of the initial discontinuity; subscript 2 designated the state on the left-hand side.

TABLE II
Initial Conditions for Test Cases

Motion	ρ_1	ρ_2	u_1	u_2	p_1	p_2
Rarefaction wave	1.0	0.59049	0	-0.5	0.71428	0.34164
Shock wave	0.59049	1.0	0	0.60622	0.47009	1.0
Contact discontinuity	1.0	0.59049	0.5	0.5	1.0	1.0

The strength of all the initial discontinuities was the same based on the two densities.

Rarefaction Wave

In a rarefaction wave, the wave speed at the head of the disturbance is greater than at the tail and, consequently, the disturbance continually widens as it propagates. This extension of the wave leads to a continual decrease in strength of the gradients and in turn to smaller and smaller truncation errors. Truncation viscosity serves no useful purpose in this motion, and as a result the schemes rank according to their formal order of accuracy.

After a sufficiently long time, the motion becomes self similar and the appropriate similarity variable for comparing results is known to be x/t . This coordinate was used to correlate numerical results taken at three different times. The results are shown in Fig. 1. The schemes are also compared on the basis of the integrated magnitude of the error signal, D , where D is defined by

$$D = \frac{1}{h} \int_0^h |(u_c - u_e)| dx,$$

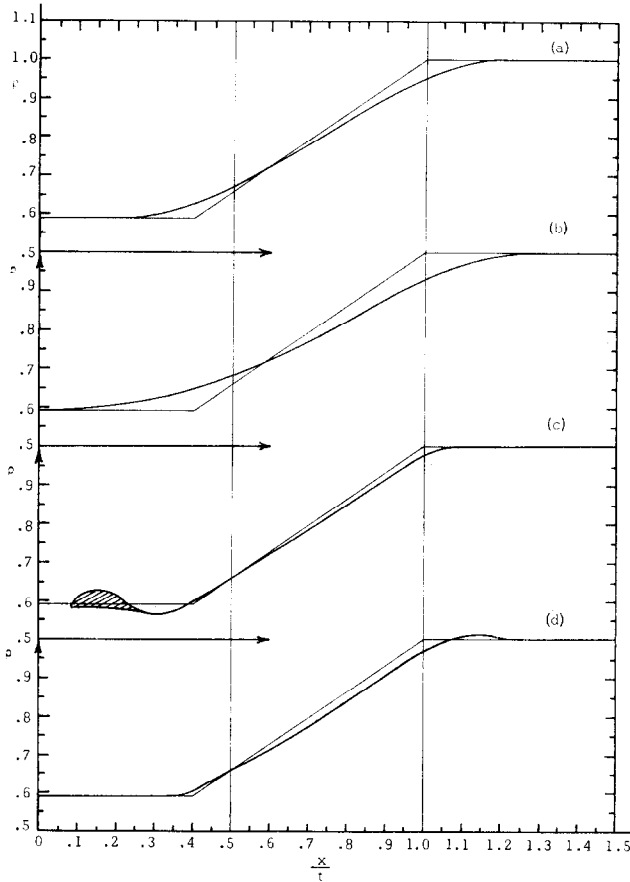


FIG. 1. Density variation through a rarefaction wave.

- Curve (a) Godunov's method, $\sigma = .95$
- Curve (b) Rusanov's method, first order, $\sigma = .95, \omega = 1.0$
- Curve (c) Richtmyer's method, $\sigma = .95$
- Curve (d) Rusanov's method, third order, $\sigma = .7, \omega = 2.0$

where

- u_o is the numerical value,
- u_e is the exact value and
- h is the distance across the wave.

These values are shown in Table III. The MLW scheme was unstable under the specified conditions, and the RLW appears much closer to the true solution than indicated by its error. The major contribution to its error signal comes from the oscillations at the tail of the disturbance. From the results it appears that for rarefaction waves the higher the order of accuracy the better the method.

TABLE III
Error Magnitudes for Inviscid Methods

Scheme	Deviation (Shock)	Deviation (Expansion)	Relative deviation (Shock)	Relative deviation (Expansion)
RLW	23.37×10^{-2}	2.08×10^{-2}	1.51	1.57
G	15.45×10^{-2}	1.72×10^{-2}	1.00	1.30
R1	16.70×10^{-2}	4.21×10^{-2}	1.08	3.18
R3	21.31×10^{-2}	1.32×10^{-2}	1.37	1.00

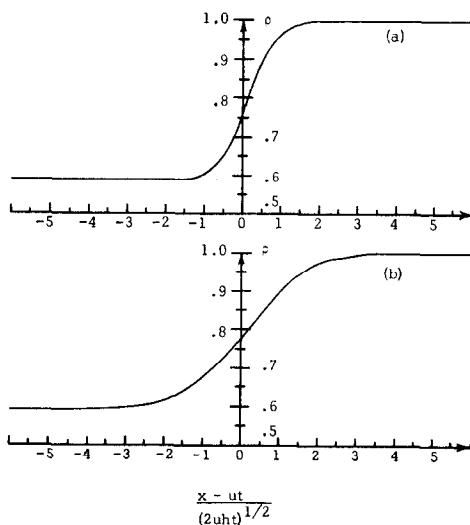


FIG. 2. Density variation through a contact discontinuity moving with velocity 0.5.
Curve (a) Godunov's method, $\sigma = .95$
Curve (b) Rusanov's method, of first order, $\sigma = .95, \omega = 1.0$

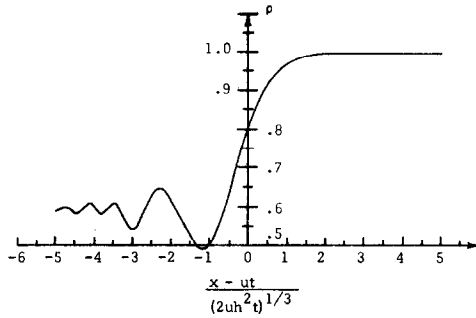


FIG. 3. Density variation through a contact discontinuity moving with velocity 0.5, computed by both Richtmyer's and McCormack's methods, $\sigma = .95$.

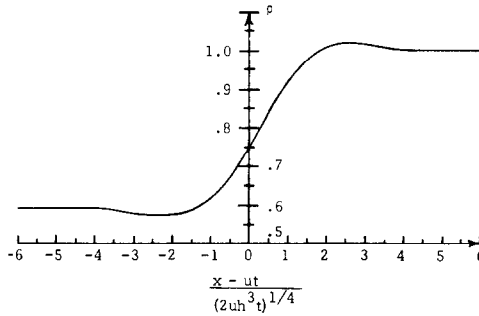


FIG. 4. Density variation through a contact discontinuity moving with velocity 0.5, computed by Rusanov's third-order method, $\sigma = .70$, $\omega = 2.0$.

Contact Discontinuity

A contact discontinuity is an interface between fluids of differing states, across which both the pressure and velocity are continuous. For an exact $1 - D$ solution the interface should be convected with an unchanging density profile at the local fluid velocity. In the numerical calculation it is smeared, however, since the density gradient is large during the early stages of motion and artificial viscosity acts to smooth the solution. This is demonstrated in the results shown in Figs. 2-4. The computational results which appear were correlated as a function of a single similarity variable, $\xi = (x - ut)/t^{1/N+1}$, where N is the order of accuracy of the scheme. It should be noted that the actual width of the smearing at large times is governed by the accuracy of the method. The higher the order, the narrower the contact discontinuity will be. For short times, it can be seen that all methods are nearly equivalent.

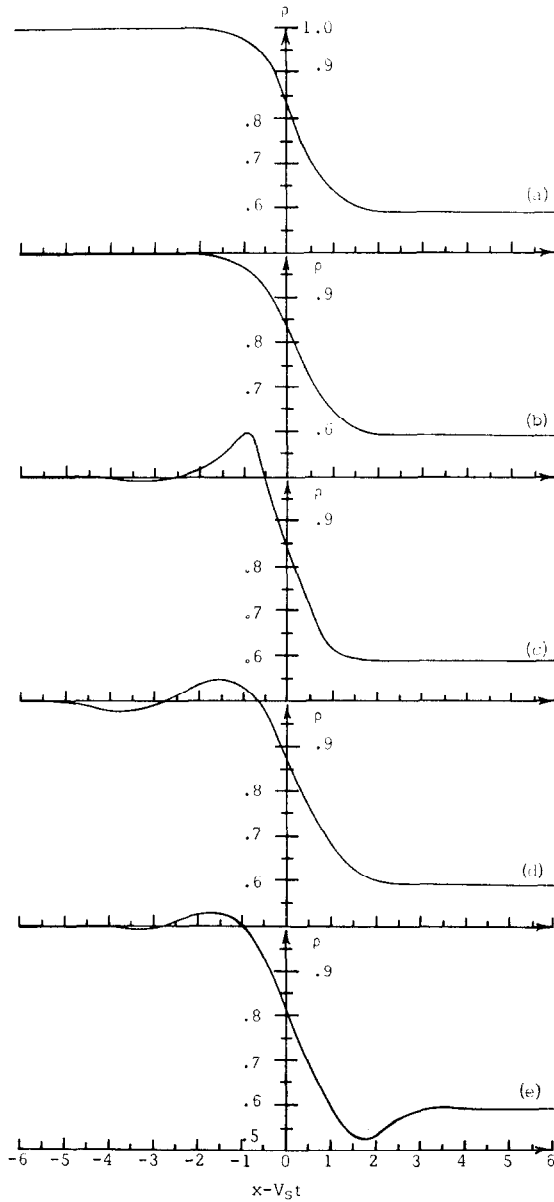


FIG. 5. Density variation through a shock wave.

- Curve (a) Godunov's method, $\sigma = .95$
- Curve (b) Rusanov's method, first order, $\sigma = .95$, $\omega = 1.0$
- Curve (c) Richtmyer's method, $\sigma = .95$
- Curve (d) McCormack's method, $\sigma = .88$
- Curve (e) Rusanov's method, third order, $\sigma = .7$, $\omega = 2.0$

Shock Wave

It is well known that shock waves are thin regions across which rapid changes in fluid state can occur. Within these regions a balance occurs between the diffusive effects of viscosity and the nonlinear steepening of wavelets. A similar phenomenon occurs in the shock smearing process employed by finite difference equations. Inside of the smeared shock a balance is established between the nonlinear effects and the truncation viscosity. The nature of the truncation viscosity was seen clearly in the previous calculation with contact surfaces.

The density profile through the shock wave calculated by each method is plotted against the running coordinate $x - V_s t$ in Fig. 5. The shock speed V_s was determined from the equation

$$V_s = \{[(p_2 - p_1)/(\rho_2 - \rho_1)] (\rho_2/\rho_1)\}^{1/2}. \quad (3)$$

Several different times are shown superimposed on the figures.

Note that all methods provide nearly the same shock width, and higher-order methods display little or no advantage. The methods were compared on the basis of their integrated error magnitude signals. The ratios of the errors are shown in Table III and are noticeably different from those found for the rarefaction wave.

2.3. *Summary of Inviscid Results*

The tests of the five differencing methods indicate that the Godunov and third-order Rusanov schemes demonstrate the greatest accuracy and seem to have the least amount of oscillations. The third-order Rusanov does not, however, propagate shocks without oscillations, while the Godunov scheme does. From the standpoint of computing time the Godunov scheme is significantly less than the third-order Rusanov method.

3. VISCOUS METHODS

Thus far the discussion has centered about solution of the inviscid or large Reynolds number flow problems. In most flows, however, are regions in which the local Reynolds number becomes small. For these flow regions real viscosity effects are important and, consequently, direct extension of inviscid differencing procedures to viscous flows can introduce error due to the artificial viscosity. It therefore is necessary to develop and optimize numerical schemes that remain stable over a wide range of local Reynolds numbers with a minimum effect of artificial viscosity. Such an optimization necessitates a study of the interaction between the artificial viscosity associated with a numerical scheme and the real viscosity of the system. The influence of time step on the stability and accuracy of the scheme is also

important, since in the time-dependent approach to steady-state problems it may be necessary to maximize the time step in order to accelerate convergence. More accuracy can generally be obtained by using second and third-order schemes; but for multidimensional problems, the equations associated with these schemes are unwieldy. However, with the introduction of the method of splitting, it is possible to “split” a multidimensional problem into a set of one-dimensional problems and take advantage of the greater accuracy of higher order schemes.

In this study, Burgers equation for a plane traveling wave of small amplitude is chosen as the model for the one-dimensional time-dependent Navier–Stokes equation. An attempt was made to extend the inviscid methods discussed earlier to approximate the inertia terms of this separation. Unfortunately, only the schemes of Rusanov were readily adaptable, since the artificial viscosity was explicit and could be controlled. As a result, the convective portion of this model was approximated by the inviscid Rusanov’s first- and third-order finite difference schemes; while the diffusive portion was differenced explicitly, implicitly or by a DuFort–Frankel scheme [13]. Linear stability analysis was used to determine the approximate range of stability of the combined schemes for various values of local Reynolds number, time step, and the artificial viscosity parameter. As a measure of the accuracy and nature of convergence of the schemes, a comparative study was made of the root-mean-square deviation of numerical results from the exact solution of Burgers equation [14–16].

3.1. Burgers Equation

Burgers equation approximates, to the first order, the motion of a plane wave of small but finite amplitude. It takes into account both convection and diffusion and is given by

$$(\partial u / \partial t) + u(\partial u / \partial x) = \delta(\partial^2 u / \partial x^2), \tag{4}$$

where δ is the diffusivity of sound, u is the excess wavelet velocity, $x = \bar{x} - c_0 t$ is a coordinate whose origin moves in the direction of the wave with the undisturbed sound speed c_0 . For the initial wave form

$$u(x, 0) = \begin{cases} u_1, & x \leq 0 \\ 0, & x \geq 0 \end{cases} \tag{5}$$

the exact solution of Eq. (4) is given by Lighthill [16] as

$$u(x, t) = \frac{u_1}{1 + \exp \left[\frac{u_1}{2\delta} \left(x - \frac{1}{2} u_1 t \right) \right]} \frac{\operatorname{erfc}(-x/2 \sqrt{\delta t})}{\operatorname{erfc}[(x - u_1 t)/2 \sqrt{\delta t}]} \tag{6}$$

This solution was used as the test case for the numerical approaches.

3.2. *Viscous Difference Approximations*

The difference approximations to Burgers equation which were tested are best explained by considering the equation in the form

$$(\partial u/\partial t) + (\partial F/\partial x) = \delta(\partial^2 u/\partial x^2), \tag{7}$$

where $F = u^2/2$.

The left side of this equation can be viewed as the inviscid form of the equation and, as a result, can be differenced by any of the inviscid methods discussed earlier. Unfortunately, this approach can introduce an artificial viscosity for stabilization which is not required when the viscous term is important. It is therefore necessary to employ inviscid schemes in which artificial viscosity can be controlled. In this study, only the two schemes of Rusanov as described in Table I were used to difference the left-hand side of Burgers equation.

The viscous term of Burgers equation was tested for three different types of differencing. The first was the standard explicit difference where

$$\partial^2 u/\partial x^2 = (u_{n+1}^{t_1} - 2u_n^{t_1} + u_{n-1}^{t_1})/\Delta x^2. \tag{8}$$

The second form was totally implicit so that the time t_1 in Eq. (8) is replaced by the

TABLE IV
Viscous Flow Difference Approximations

Inertia terms	Viscous terms	Stability condition
1st-order Rusanov	$\begin{cases} \text{Explicit} - (u_{m+1}^n - 2u_m^n + u_{m-1}^n) \\ \text{Implicit} - (u_{m+1}^{n+1} - 2u_m^{n+1} + u_{m-1}^{n+1}) \end{cases}$	$\begin{aligned} \sigma^2 &\leq 2\xi + \omega\sigma \leq 1 \\ \sigma^2 &\leq 2\xi + \omega\sigma \leq 1 + 4\xi \\ \xi &= q/\text{Re} \end{aligned}$
3D-order Rusanov		
Step I	$\begin{cases} \text{Explicit} - 0 \\ \text{Implicit} - 0 \\ \text{DuFort-Frankel} - 0 \end{cases}$	(See figures in text)
Step II	$\begin{cases} \text{Explicit} - 0 \\ \text{Implicit} - 0 \\ \text{DuFort-Frankel} - (8q/3 \text{ Re})(u_{m+1/2}^{(1)} - u_m^{(a)} - u_m^n + u_{m-1/2}^{(1)}) \end{cases}$	
Step III	$\begin{cases} \text{Explicit} - (q/\text{Re})(u_{m+1}^n - 2u_m^n + u_{m-1}^n) \\ \text{Implicit} - (q/\text{Re})(u_{m+1}^{n+1} - 2u_m^{n+1} + u_{m-1}^{n+1}) \\ \text{DuFort-Frankel} - (q/\text{Re})[u_{m+1}^{(2)} - (4/3)u_m^{n+1} - (2/3)u_m^n + u_{m-1}^{(2)}] \end{cases}$	

final time t_2 . The third scheme was the DuFort-Frankel approach which has the form

$$\partial^2 u / \partial x^2 = [u_{n+1}^{\bar{t}} - (4/3) u_n^{t_2} - (2/3) u_n^{t_1} + u_{n-1}^{\bar{t}}] / \Delta x^2. \quad (9)$$

In this expression t_2 is the final time, t_1 is the initial time and \bar{t} is a time between t_1 and t_2 . As a result of this form a predictor difference equation is required to obtain the values of u at the time \bar{t} . The predictor equation which is usually of lower-order accuracy than the final equation, can be formed in two ways. If one is interested only in steady-state results, the first is to neglect the viscous term and employ only the explicit inertia difference equation as the predictor. For a more

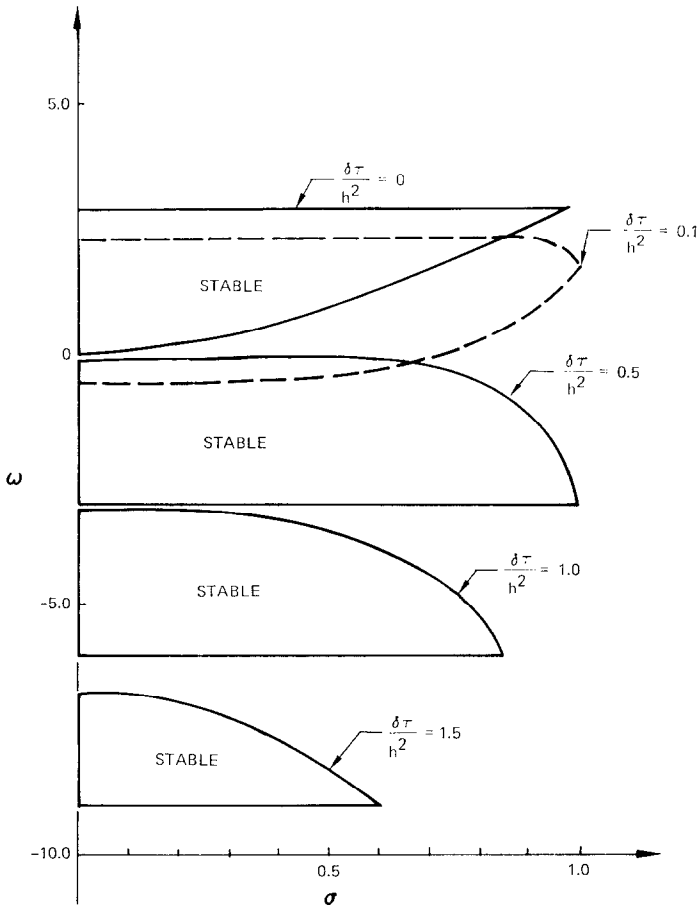


FIG. 6. Stability regions for 3rd-order Rusanov (explicit).

exact predictor one can use a total explicit difference form of Burgers equation. Both of these approaches were tested with the third-order Rusanov differencing. For the 1st-order Rusanov inertia scheme these tests become redundant due to the order of the scheme and therefore the DuFort–Frankel method was not tested.

The complete difference approximations as they were used in the computations

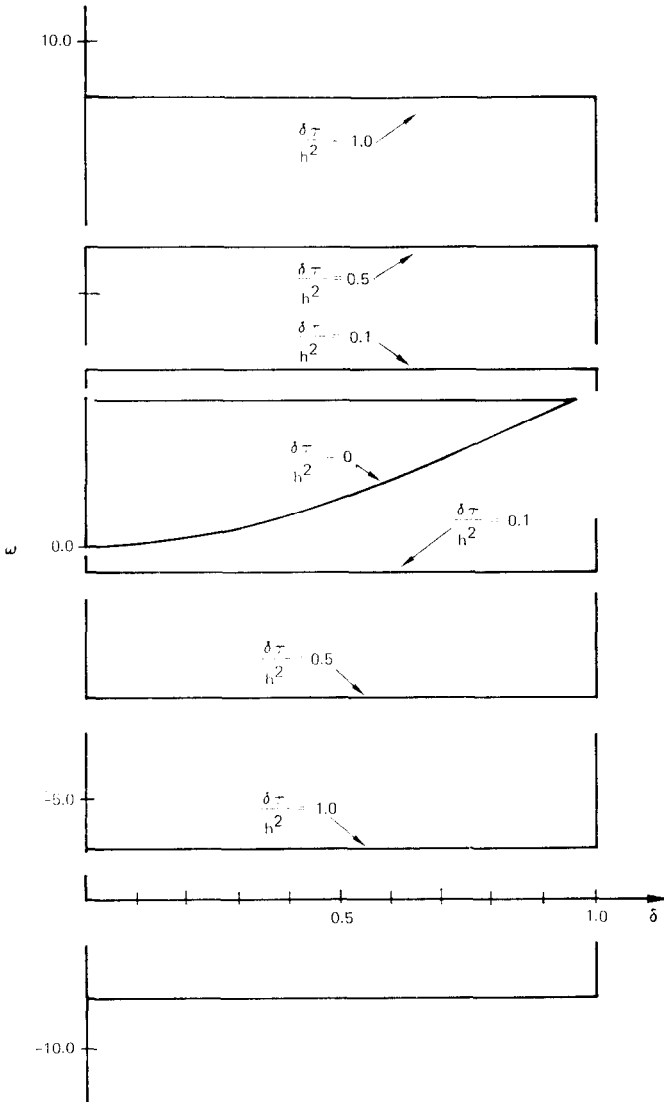


FIG. 7. Stability regions for 3rd-order Rusanov (implicit).

are listed in Table IV along with the linear stability criteria. The schemes developed using the first-order Rusanov method yielded stability conditions that could be solved analytically, but the stability regions for the third-order case had to be obtained by a computer study. Stability results from the study are shown in Figs. 6–9. The results are displayed as enclosed or bracketed regions within which stable solutions are obtained. Note that for the explicit scheme the region of stability in the (ω, σ) plane decreases as $(\delta\tau/h^2)$ increases. For the implicit and DuFort–Frankel schemes the stability region increases in area as $(\delta\tau/h^2)$ increases.

The test calculations for comparison with the exact solution to Burgers equation were conducted subject to the stability criteria presented for each scheme. The results of these tests will now be discussed.

3.3. Calculation Results

The numerical methods which have been presented were utilized to compute the solution to Burgers equation for the initial conditions

$$u(x, 0) = \begin{cases} 1 & \text{for } x < 0 \\ 0 & \text{for } x > 0. \end{cases}$$

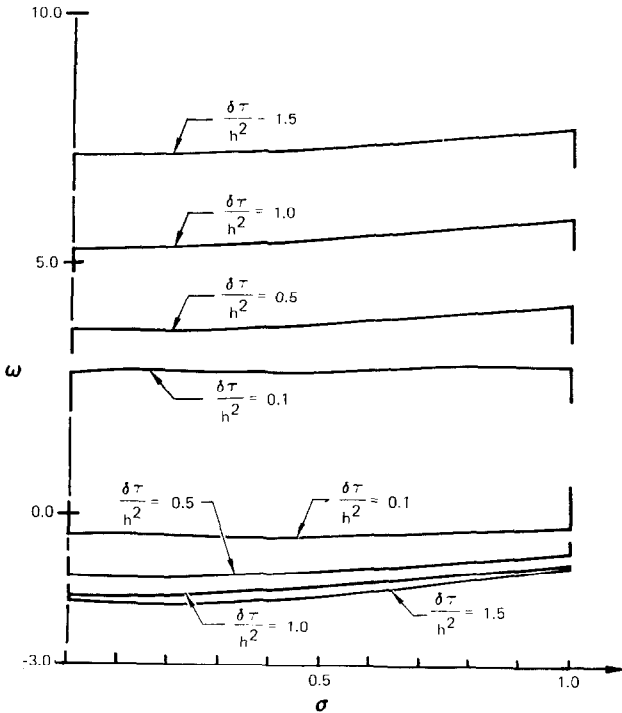


FIG. 8. Stability regions for 3rd-order Rusanov (DuFort–Frankel/DuFort–Frankel).

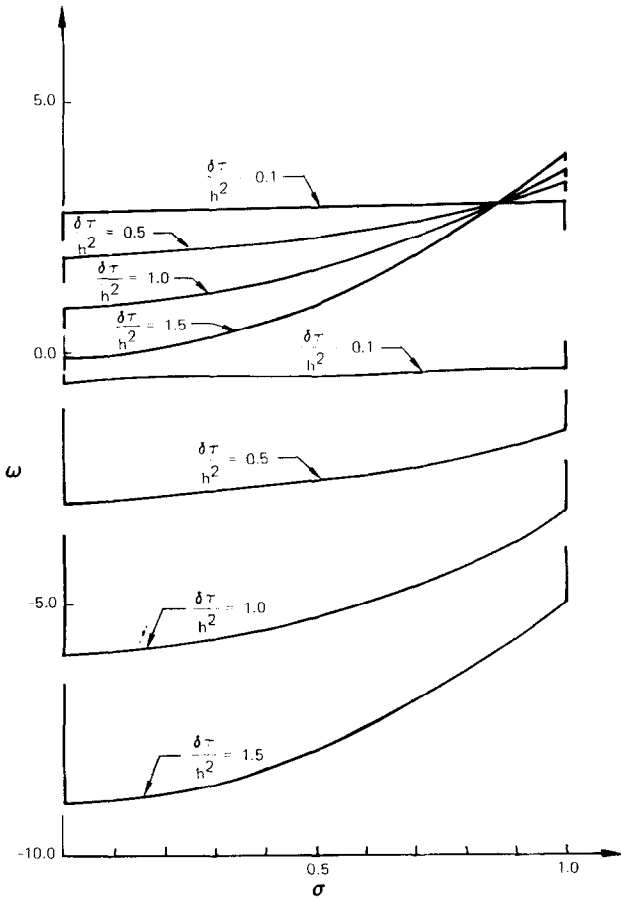


FIG. 9. Stability regions for 3rd-order Rusanov (DuFort-Frankel).

The schemes with implicit differencing of the diffusion term were solved by the Double-Sweep method [17], while all other schemes are solved by the usual method of direct substitution from the previous time level.

A grid size, $h = 0.01$ was chosen; and τ/h varied within the range $0 < (\tau/h) \leq 1$.

For $\omega = 1$, $\tau/h = 0.2$, and $0.1 \leq (h/\delta) \leq 10^6$, all the schemes were integrated through 200 cycles. Within this time the initial wave form evolved into a steady state profile moving in the positive n -direction with a mean shock speed, $V_s = 0.5$.

The computed velocity profiles are compared with the exact solutions in Fig. (10) for various values of (h/δ) . These results were evaluated by computing the root-mean-square deviation between the numerical scheme prediction and the exact solution.

The root-mean derivation, Ω , is defined by the relation

$$\Omega = \sqrt{\frac{\sum^N d_m^2}{(N - 1)}}$$

where

- $d_m = u_m - u_m^*$,
- $N =$ total number of computed points,
- $u_m =$ computed values,
- $u_m^* =$ exact values.

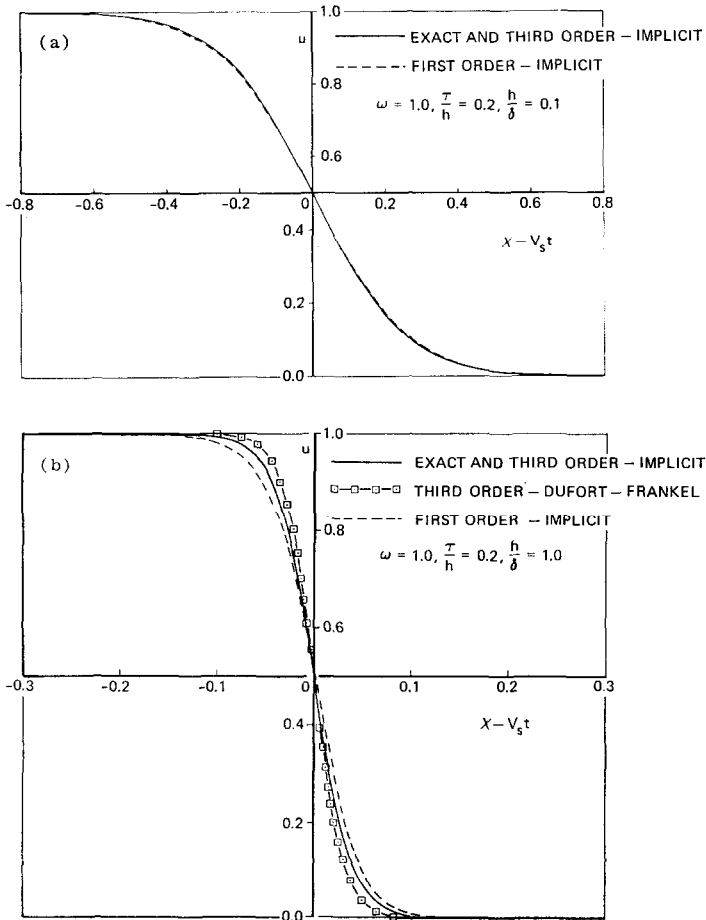


FIGURE 10.

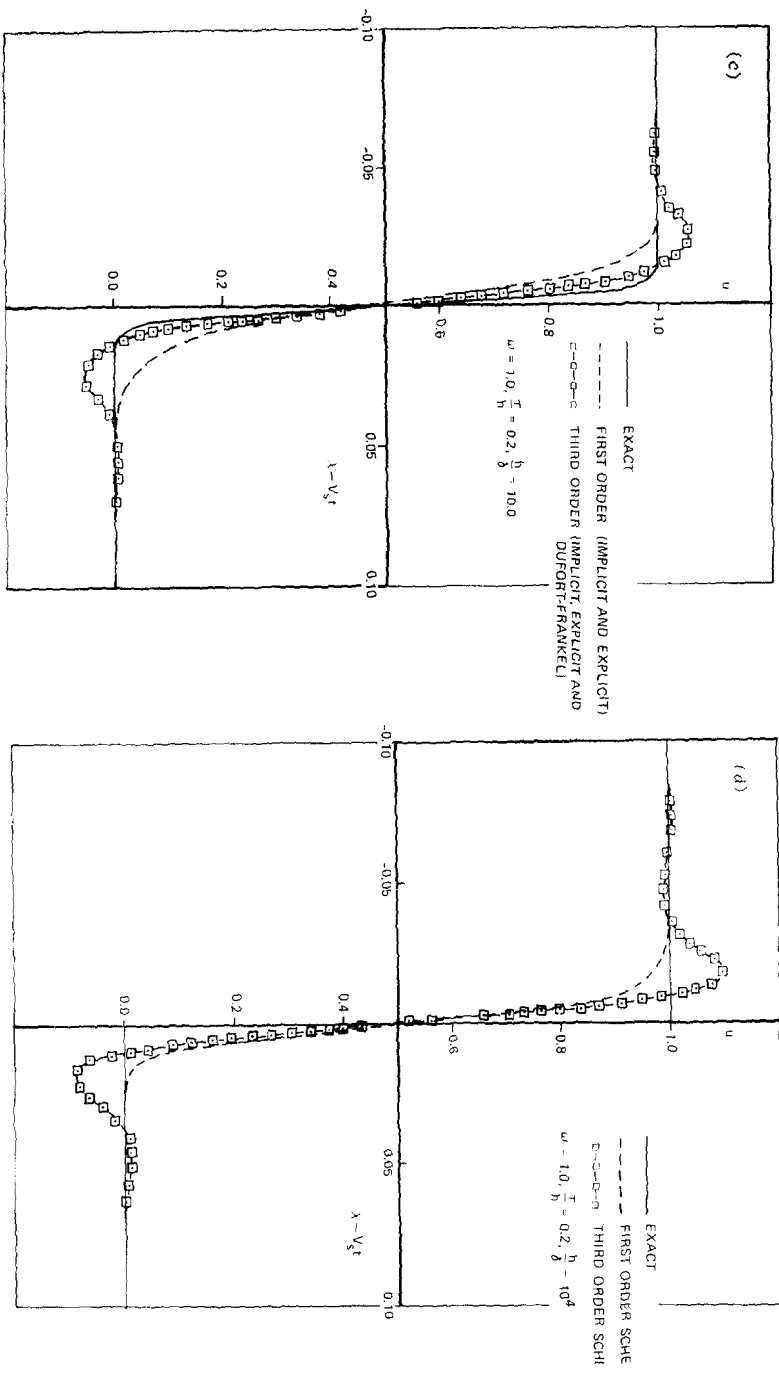


FIG. 10. a, b, c, d. Comparison of exact solutions with numerical solutions of Burgers equation.

The variation of Ω with (h/δ) for each scheme is plotted in Fig. 11. From the results it is clear that the most accurate method is the implicit viscous third-order Rusanov scheme. Upon determining this fact the combined scheme was studied to determine the effect of the artificial viscosity on the accuracy. These results are shown in Fig. 12. From these results it is clear that the artificial viscosity can significantly affect the accuracy for a Reynolds number between 0.5 and 10. It appears, however, that $\omega = 1$ is a good value to employ to satisfy both the overall accuracy and stability conditions.

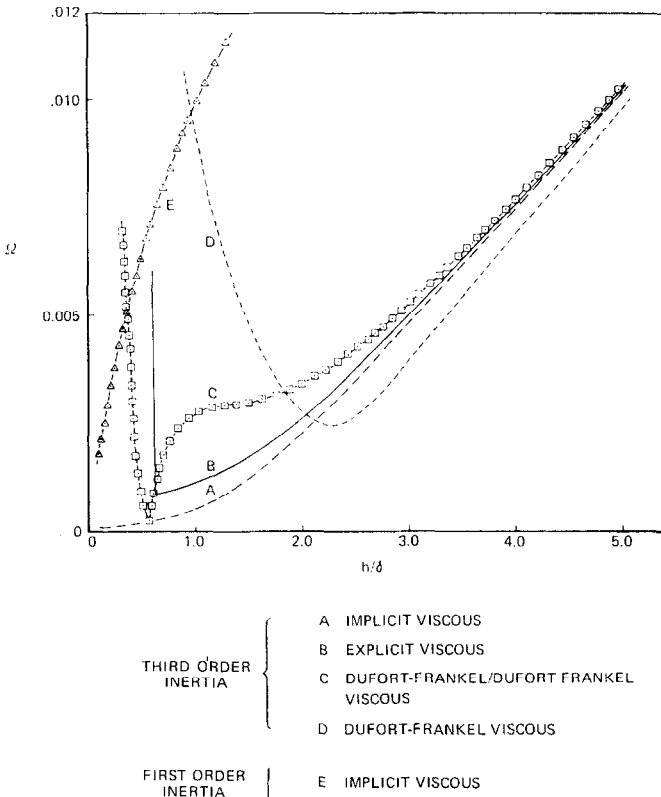


FIG. 11. Root-mean-square error between exact and numerical solutions as a function of h/δ .

4. CONCLUSIONS

The study of the viscous and inviscid methods has provided some interesting information on both types of methods. For inviscid flows it appears that the first-

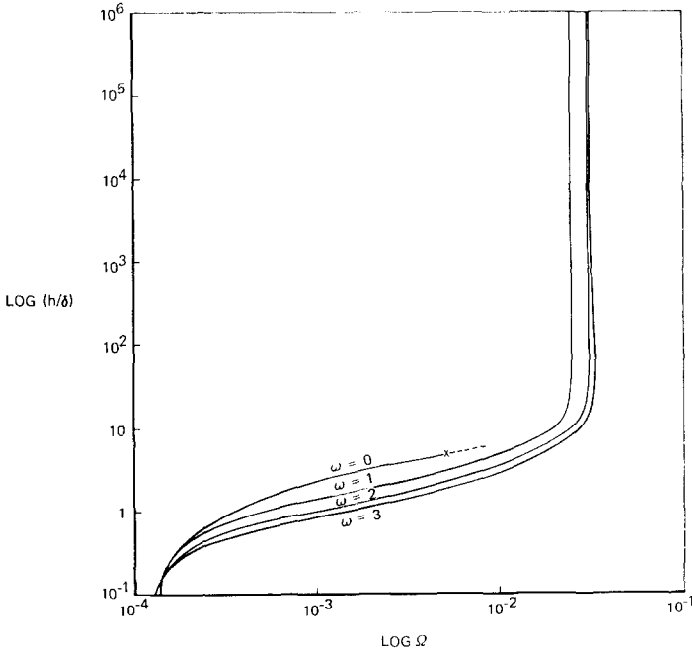


FIG. 12. Root-mean-square error for the implicit viscous 3rd-order Rusanov scheme.

and third-order methods offer the best overall accuracy. For first-order calculations the method of Godunov appears to have the least error when compared to the first-order Rusanov scheme. The third-order method of Rusanov appears, however, to yield the most accurate inviscid calculations. It unfortunately has the disadvantage of requiring almost twice the amount of computer time as the first-order schemes.

For viscous flows it appears that implicit differencing of the viscous terms is preferable to explicit or DuFort–Frankel differencing. For the inertial terms any scheme which is stable for inviscid flows, and has controllable artificial viscosity at low Reynolds numbers may be used. The third-order scheme of Rusanov appears preferable at this time since the artificial viscosity is of the order of the step size to the fourth power and hence the artificial viscosity can be maintained small for reasonable step size. For lower order schemes it becomes necessary to reduce the artificial viscosity with the Reynolds in order to make the schemes acceptable for Reynolds numbers less than one.

REFERENCES

1. K. A. BAGRINOVSKII AND S. K. GODUNOV, Difference methods for multidimensional problems, *Dokl. AN SSSR*, **115** (1951), 431.
2. N. N. YANENKO, "Method of fractional steps for solution of multidimensional problems of mathematical physics," Academy of Sciences SSR, Siberian Division, Novosibirski, 1967.
3. T. D. TAYLOR AND E. NDEFO, "Computation of viscous flow in a channel by the method of splitting," Second International Conf. on Numerical Methods, Berkeley, 1970.
4. A. F. EMERY, An evaluation of several differencing methods for inviscid fluid flow problems, *J. Comput. Phys.* **2** (1968), 306.
5. P. D. LAX, "Weak solutions of nonlinear hyperbolic equations and their numerical computation," *Commun. Pure Appl. Math.* **7** (1954), 159.
6. V. V. RUSANOV, Calculation of interaction of non-steady shock waves with obstacles, National Research Council of Canada Technical Translation 1027, *Zhor, Nych. Mat. I Mat.* **1** (1961), 267.
7. H. J. LONGLEY, "Methods of Differencing in Eulerian Hydrodynamics, LAMS-2379, Los Alamos Scientific Laboratory, N.M., 1960.
8. P. D. LAX AND B. WENDROFF, "Difference schemes with high order of accuracy for solving hyperbolic equations," NYU Report 9759, Courant Inst. of Math. Sci., New York University, July, 1962.
9. R. D. RICHTMYER, "A Survey of Difference Methods for Non-Steady Fluid Dynamics," NCAR Technical Notes 63-2, National Center for Atmospheric Research, Boulder, Col., 1962.
10. S. K. GODUNOV, Finite difference method for numerical computation of discontinuous solutions of the equations of fluid dynamics, tr. I. Bohachevsky, *Math. Sb.* **47** (89) (1959), 271.
11. R. W. MACCORMACK, "The Effect of Viscosity in Hypervelocity Impact Cratering," AIAA Hypervelocity Impace Conference, Cincinnati, OH, 1969.
12. V. V. RUSANOV, Difference schemes of third order accuracy for 'Across' — computation of discontinuous solutions, *Fluid Dyn. Trans.* **4** Warsaw, (1969), 285.
13. R. D. RICHTMYER, "Difference Methods for Initial Value Problems," Interscience, New York, 1957.
14. E. HOPF, The partial differential equation $u_t + uu_x = \mu u_{xx}$, *Comm. Pure Appl. Math.* **3** (1950), 201.
15. J. D. COLE, On a quasilinear equation occurring in aerodynamics, *Quart. Appl. Math.* **9** (1951), 225.
16. M. J. LIGHTHILL, "Viscosity Effects in Sound Waves of Finite Amplitude," in "Surveys in Mechanics," (G. K. Batchelor and R. M. Davies, Eds.) Cambridge University Press, 1956, 250.
17. S. K. GODUNOV AND V. S. RYABENKI, "Theory of Difference Schemes," North-Holland Publishing Co., Amsterdam, 1964.